Turkish Computational and Theoretical Chemistry

Turkish Comp Theo Chem (TC&TC)

Volume(Issue): 9(5) – Year: 2025 – Pages: 62-76

e-ISSN: 2602-3237

https://doi.org/10.33435/tcandtc.1708573

Received: 29.05.2025 ***Accepted:*** 05.06.2025 *Research Article*

Computational Investigation of Octanediamide Derivatives as Potential Inhibitors of Monkeypox Virus: HF and Molecular Docking Approaches

Gamze Tüzün[a,1], Koray Sayın[a], Burak Tüzün[b]

[a]Department of Chemistry, Faculty of Science, Sivas Cumhuriyet University, Sivas, 58140, Turkey Sivas, Turkey

[b]Plant and Animal Production Department, Technical Sciences Vocational School of Sivas, Sivas Cumhuriyet University, Sivas, Turkey

Abstract: In this study, the electronic structure, reactivity, molecular docking interactions, and pharmacokinetic properties of eight different octanediamide derivative compounds were investigated to evaluate their potential as antiviral agents against the monkeypox virus (MPXV). Quantum chemical parameters such as HOMO-LUMO energy levels, energy gap (ΔE), chemical hardness, softness, electronegativity, chemical potential, electrophilicity index, and dipole moment were calculated at the HF/6-31++G(d,p) level using Gaussian 09. The docking behaviors of the molecules were evaluated via the Schrödinger Maestro platform against two critical monkeypox virus proteins (PDB IDs: 2V54 and 6BED). In parallel, ADME/T predictions were performed using the QikProp module to evaluate their drug-likeness and pharmacokinetic suitability. Results revealed that molecule 7 was the most reactive and electrophilic compound, while molecule 4 demonstrated the greatest electronic stability. Docking analysis indicated that molecule 5 and 8 displayed the strongest binding interactions with MPXV proteins. Furthermore, molecule 3 exhibited the most favorable ADME profile with high membrane permeability and acceptable solubility. These findings suggest that several of the studied compounds, particularly molecules 3, 5, 7, and 8, are promising antiviral candidates for further in vitro and in vivo evaluation against monkeypox virus.

Keywords: Monkeypox virus, Molecular docking, DFT, Drug

1. Introduction

Monkeypox virus (Mpox; MPXV) is a double-stranded DNA virus belonging to the Orthopoxvirus genus of the Poxviridae family, zoonotic in nature and capable of causing serious infections in humans [1]. This virus is genetically very similar to the variola virus and was first identified in laboratory monkeys in 1958, with the first human case reported in the Democratic Republic of the Congo in 1970 [2]. Although it was initially limited to a zoonotic disease specific to West and Central Africa, it caused simultaneous outbreaks in many countries in 2022 and was defined as a global threat to international public health [3].

Although the natural reservoirs of monkeypox virus have not been precisely determined, rodents (especially squirrels and rats) are considered the main reservoirs. Transmission to humans occurs through direct contact with infected animals, body fluids, skin lesions or contaminated materials. In addition, it has been determined that skin contact, close social relationships and human-to-human transmission via respiratory droplets are also important in recent outbreaks [4].

MPXV carries a large genome of approximately 197 kilobases and is one of the rare DNA viruses that replicate in the cytoplasm rather than in the host cell nucleus. Its genome encodes hundreds of genes related to DNA replication, transcription, immune modulation, and structural protein production. This virus produces a large number of immunomodulatory proteins to evade the host immune system [5]. These proteins inhibit the type

[1] Corresponding Authors

e-mail: gamzekekul@gmail.com

I interferon response, suppress NK cell activity, and modulate cytokine responses. In addition, the virus has two different infectious forms, EEV (extracellular enveloped virion) and IMV (intracellular mature virion). These forms offer important strategies for cell-to-cell spread and evasion of host immunity. At the chemical and molecular level, the structural proteins of MPXV (especially glycoproteins such as A27L, B5R, L1R) play a critical role in the entry of the virus into the cell and its escape from the immune response [6]. These protein structures are important molecules in terms of antiviral drug targeting and vaccine development studies. In recent years, molecular docking and dynamic simulation studies on these proteins have enabled the identification of effective inhibitor compounds [7]. For example, the antiviral agent called tecovirimat (ST-246) inhibits viral exit by interacting with the B5R protein and is the first FDA-approved Mpox treatment. In addition, nucleotide analogs such as cidofovir and brincidofovir are also potential DNA polymerase-targeted treatments. Studies conducted with in silico methods play a critical role in the preliminary screening of potential drug candidates by modeling the three-dimensional structures of viral proteins, determining drug binding sites, and ADME/T (absorption, distribution, metabolism, elimination, and toxicity) analyses [8,9]. In this context, molecular modeling software such as Schrödinger, AutoDock, and MOE are used. Targeting proteins that play a role in host cell interaction, especially A28L and D13L, forms the basis of new generation antiviral strategies.

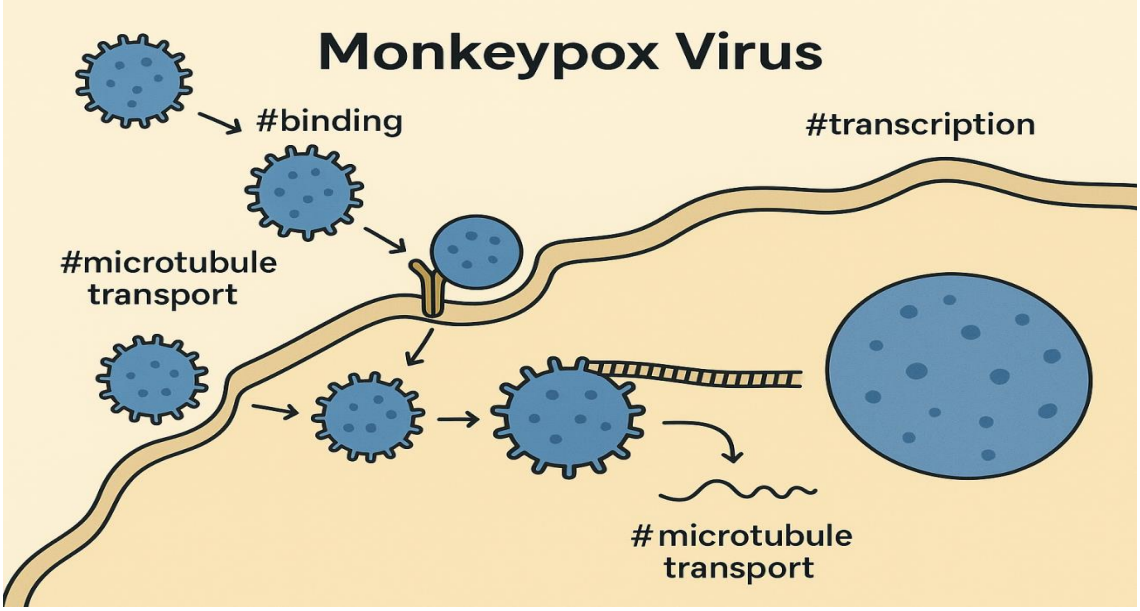

Figure 1. movement of monkeypox virus in cells

Monkeypox virus (MPXV) is a large virus with an envelope structure, containing double-stranded DNA, and is one of the rare DNA viruses that completes its replication in the cytoplasm after entering the infected cell [10]. The process of entering the cell begins with the interaction of specific glycoproteins on the surface of the virus with target receptors on the host cell membrane. These receptors include heparan sulfate and some cell adhesion molecules. After the virus binds to the host cell membrane, it is taken into the cell by fusing with the membrane or by endocytosis. After entering the cell, the viral envelope is broken down by the effect of low pH and enzymes in the endosomal environment and the viral structures are released into the cytoplasm without going to the nucleus [11]. This event is called uncoating, or peeling off of the viral capsid.

The transportation of viral structures within the cell occurs via the cell's cytoskeleton system. The virus moves within the cytoplasm, especially through microtubules and motor proteins such as dynein or kinesin attached to them. As a result of this transportation, the virus is directed to suitable cytoplasmic regions for replication and gene expression [12]. Since monkeypox virus carries its

own RNA polymerase, it can directly initiate the transcription process in the cytoplasm without entering the host nucleus. First, early genes are transcribed and these gene products suppress the host immune response and prepare the environment for viral replication. Then, late and late-late stage genes are activated; these genes code for viral capsid proteins and membrane proteins [13].

In the cytoplasm, special structures called "viral factories" are formed. In these structures, viral DNA replication is carried out, new RNA transcripts are produced and protein synthesis is coordinated. Replication is carried out with the help of DNA polymerase and helicase enzymes encoded by the virus [14]. The new DNA molecules and structural proteins produced are used for the assembly of new virions. In the final stage, newly formed virus particles are directed to the cell membrane and released outside the cell by lysis or exocytotic means, thus continuing the infection cycle.

All these processes; It involves complex chemical and biological events such as protein-protein interactions, pH changes, cytoskeletal transport mechanisms, enzymatic reactions and suppression of host immune responses [15]. Therefore, the intracellular behavior of Monkeypox virus is of critical importance for modern virological research and antiviral drug development studies. In particular, understanding the viral entry mechanisms and intracellular transport pathways forms the basis for the development of next-generation targeted treatment strategies.

In this study, molecule 1 (S)-N1-(6-(2-naphthamido)-4,5,6,7-tetrahydrobenzo[d]thiazol-2-yl)-N8-hydroxyoctanediamide, molecule 2 (S)-N1-hydroxy-N8-(6-(4-(trifluoromethoxy)benzamido)-4,5,6,7-tetrahydrobenzo[d]thiazol-2-yl)octanediamide, molecule 3 (S)-N1-hydroxy-N8-(6-(3,4,5-trimethoxybenzamido)-4,5,6,7-tetrahydrobenzo[d]thiazol-2-yl)octanediamide, molecule 4 (S)-N1-(6-(3-chlorobenzamido)-4,5,6,7-tetrahydrobenzo[d] thiazol-2-yl)-N8-hydroxyoctanediamide, molecule 5 (S)-N1-(6-([1,1′ -biphenyl]-4-carboxamido)-4,5,6,7-tetrahydrobenzo[d]thiazol-2-yl)-N8-hydroxyoctanediamide, molecule 6 (S)-N1-(6-(3,5-dimethylbenzamido)-4,5,6,7-tetrahydrobenzo[d] thiazol-2-yl)-N8-hydroxyoctanediamide, molecule 7 (S)-N1-hydroxy-N8-(6-(3-(trifluoromethyl)benzamido)-4,5,6,7-tetrahydrobenzo[d]thiazol-2-yl)octanediamide, molecule 8 (S)-N1-(6-([1,1′ -biphenyl]-3-carboxamido)-4,5,6,7-tetrahydrobenzo[d]thiazol-2-yl)-N8-hydroxyoctanediamide molecules were all synthesized by Sun and co-worker [16] in Figure 1. Then, the quantum chemical parameters of these molecules were calculated with the Gaussian package program. Calculations using the 6-31++g(d,p) basis set in the HF [17] techniques were performed using these programs. Then, the activities of the molecules against various proteins, which are PDB ID: 2V54 [18] and 6BED [19] proteins, were compared. Finally, the drug properties of the molecules were examined by ADME/T analysis of the molecules.

2. Computational Method

The chemical and biological properties of molecules can be significantly deduced from theoretical computations. Theoretical simulations yield extensive insights on quantum chemical parameters. The calculated parameters elucidate the chemical reactivity of the compounds. Molecules are computed utilizing several applications. Gaussian09 RevD.01 and GaussView 6.0 are the designations of these distinct apps [20,21]. Calculations employing the 6-31++g(d,p) basis set with the HF methods was conducted utilizing these programs. Numerous quantum chemical parameters have been identified by these quantum chemistry calculations. The subsequent presentation illustrates the calculated parameters, each representing a unique molecular chemical characteristic [22,23]. The equations for determining these parameters are shown in equations.

$$\chi = -\left(\frac{\partial \mathrm{E}}{\partial \mathrm{N}}\right)_{\upsilon(r)} = \frac{1}{2}(I + A) \cong \frac{1}{2}(E_{HOMO} + E_{LUMO})$$

$$\eta = -\left(\frac{\partial^2 \mathrm{E}}{\partial \mathrm{N}^2}\right)_{\upsilon(r)} = \frac{1}{2}(I - A) \cong -\frac{1}{2}(E_{HOMO} - E_{LUMO})$$

$$\sigma = 1/\eta \qquad \omega = \chi^2/2\eta \qquad \varepsilon = 1/\omega$$

Molecular docking calculations are employed to compare the biological activities of molecules with biological materials. Molecular docking computations were conducted utilizing Schrödinger's Maestro Molecular modeling

platform (version 13.4) [24]. Calculations encompass multiple phases. Each phase is executed distinctly. Proteins were synthesized in the initial phase utilizing the protein preparation module [25]. The active sites of the proteins were found in this module. The subsequent phase entails the preparation of the compounds under investigation. The LigPrep module [26] is prepared for computations using optimized structures once the molecules have been initially optimized in the Gaussian software application. Subsequent to preparation, the interactions between the compounds and the cancer protein were examined utilizing the Glide ligand docking module [27,28]. All calculations were executed with the OPLS4 methodology. The pharmacological potential of the examined substances will be assessed using ADME/T study (absorption, distribution, metabolism, excretion, and toxicity). The impacts and responses of substances in human metabolism were forecasted utilizing the Qik-prop module of Schrödinger program [29].

3. Results and discussion

In order to get a comprehensive understanding of the electronic structure and chemical characteristics of molecules, it is crucial to have a sound understanding of various terminologies, including the ΔE energy gap, E_{HOMO}, E_{LUMO}, chemical hardness, softness, electronegativity, and chemical potential [30]. A chemical's stability and reactivity may be evaluated based on these basic characteristics, which are used to evaluate the chemical.

The energy gap, often known as ΔE, is a measurement that measures the difference in energy levels that exist between the highest occupied molecular orbital (HOMO) of a molecule and the lowest unoccupied molecular orbital (LUMO) of the same molecule [31]. It is necessary to have a thorough comprehension of this value in order to have a complete grasp of the electrical stability and reactivity of a molecule. When the ΔE value is larger, it indicates that the structure of the molecule is more stable, whereas when the ΔE value is less, it indicates that the molecular reactivity is increased [32].

When discussing the energy of molecular orbitals, the terms E_{HOMO} and E_{LUMO} are used to refer to the energy of the molecular orbital with the highest occupied energy and the molecular orbital with the lowest unoccupied energy, respectively. The LUMO is a measure of a molecule's ability to take in electrons, which is indicative of electrophilic behavior. On the other hand, the HOMO is responsible for determining a molecule's tendency to donate electrons, which is indicative of nucleophilic activity [33]. It is necessary to have a full understanding of the energy difference between the HOMO and LUMO states in order to comprehend the mechanics of electron transport when chemical reactions are being carried out.

Chemical hardness is the ability of a molecule to withstand changes that are brought about by influences that are external to the molecule. There is a decrease in reactivity and an increase in structural stability in molecules that are more stiff. The reactivity of a molecule may be quantified using the concept of chemical softness; molecules that are softer are more susceptible to changes in their chemical structure. In order to better understand the acid-base characteristics of molecules and to make predictions about the formation of chemical bonds, the notions of softness and hardness may be of assistance [34].

The polarity of chemical bonds is mostly determined by electronegativity, which is an important factor. One might use this expression to refer to the propensity of an atom or molecule to attract electrons that are involved in bonding. In the context of chemical reactions, compounds that have a higher electronegativity are more efficient in attracting electrons and displaying electrophilic properties.

The change in energy that occurs inside a molecule may be quantified using chemical potential, which also provides an indication of how the system reacts to changes in electron density [31]. As an important indication for determining the molecule stability and reaction energy, this number is a key indicator. The integration of these principles results in the establishment of a complete foundation for understanding the electrical structure, stability, and chemical reactivity of molecules. The evaluation of the energy levels of the HOMO and LUMO states, in combination with the ΔE, provides a good tool for forecasting the chemical reactivity of a substance. For the purpose of grasping molecular reactions to external stimuli, it is essential to have an understanding of characteristics like as

electronegativity, malleability, and chemical hardness. In Table 1 and Figure 2, each and every factor is listed in exhaustive detail respectively.

Table 1. The calculated quantum chemical parameters of molecules.

	E_{HOMO}	E_{LUMO}	I	A	ΔE	η	μ	χ	PA	ω	ε	dipol	Energy
HF/6-31++g(d,p) LEVEL													
1	-8.1798	0.9241	8.1798	-0.9241	9.1039	4.5520	0.2197	3.6279	-3.6279	1.4457	0.6917	3.9192	-52148.0238
2	-8.5210	0.8580	8.5210	-0.8580	9.3790	4.6895	0.2132	3.8315	-3.8315	1.5653	0.6389	3.8555	-57129.3047
3	-8.4146	0.9851	8.4146	-0.9851	9.3997	4.6999	0.2128	3.7148	-3.7148	1.4681	0.6812	3.2211	-54107.4560
4	-8.4710	0.9706	8.4710	-0.9706	9.4416	4.7208	0.2118	3.7502	-3.7502	1.4896	0.6713	3.1351	-60483.8909
5	-8.4068	0.9472	8.4068	-0.9472	9.3540	4.6770	0.2138	3.7298	-3.7298	1.4872	0.6724	4.5666	-54240.8896
6	-8.4089	0.9407	8.4089	-0.9407	9.3496	4.6748	0.2139	3.7341	-3.7341	1.4914	0.6705	6.1349	-50119.5402
7	-8.5681	0.6267	8.5681	-0.6267	9.1948	4.5974	0.2175	3.9707	-3.9707	1.7147	0.5832	4.0709	-58140.7010
8	-8.4068	0.9472	8.4068	-0.9472	9.3540	4.6770	0.2138	3.7298	-3.7298	1.4872	0.6724	4.5650	-54240.8824

The Koopman theorem [35], which is a fundamental premise in the field of molecular orbital theory, establishes a correlation between the electron affinity and ionization energy of a molecule and its HOMO and LUMO energy levels. In accordance with the idea, the energy of the HOMO is equivalent to the ionization energy of the molecule, while the energy of the LUMO is a reflection of the electron affinity of the molecule. In this manner, a reliable instrument is provided for the purpose of predicting the electrical properties and reactivity of molecules. Given that the theory does not take into account electron-electron interactions, the results are little more than speculations that could need for more complex calculations in order to discover a way to validate them.

Elucidating acid-base chemistry was the motivation for the development of the Hard and Soft Acid-Base (HSAB) paradigm [36]. From this point of view, it is hypothesized that hard acids have powerful interactions with hard bases, while soft acids are able to establish strong links with soft bases [37]. This theory proposes that a system commonly takes a structure with increased hardness as a result of its increased stability and less reactivity compared to other structures. It is possible to make accurate predictions about the stability of molecules and chemical processes by using this concept as a foundation. The idea of maximal hardness [38] is used rather often, particularly in the process of assessing transition states and producing reactive intermediates.

This comprehensive understanding of the qualities of molecular bonding and reactivity may be achieved by the application of these three essential ideas, which provide both a theoretical and practical basis. The HSAB principle sheds light on the properties of acid-base interfaces [39], Koopman's theorem investigates the paths that electrons take to go from one location to another, and PMH primarily anticipates the stability of molecules [40]. It is possible that a thorough knowledge of the behavior of chemical systems might be obtained via the combination of different techniques.

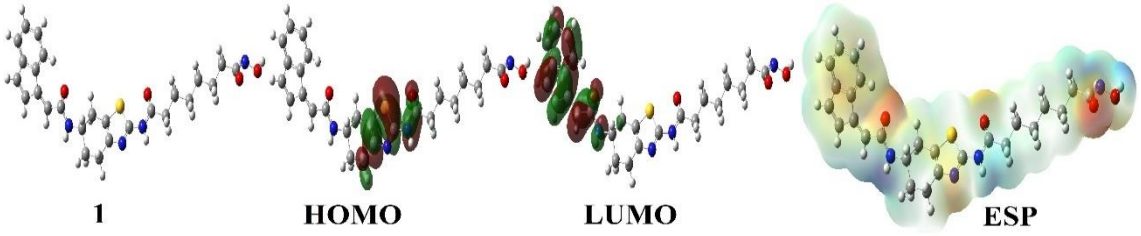

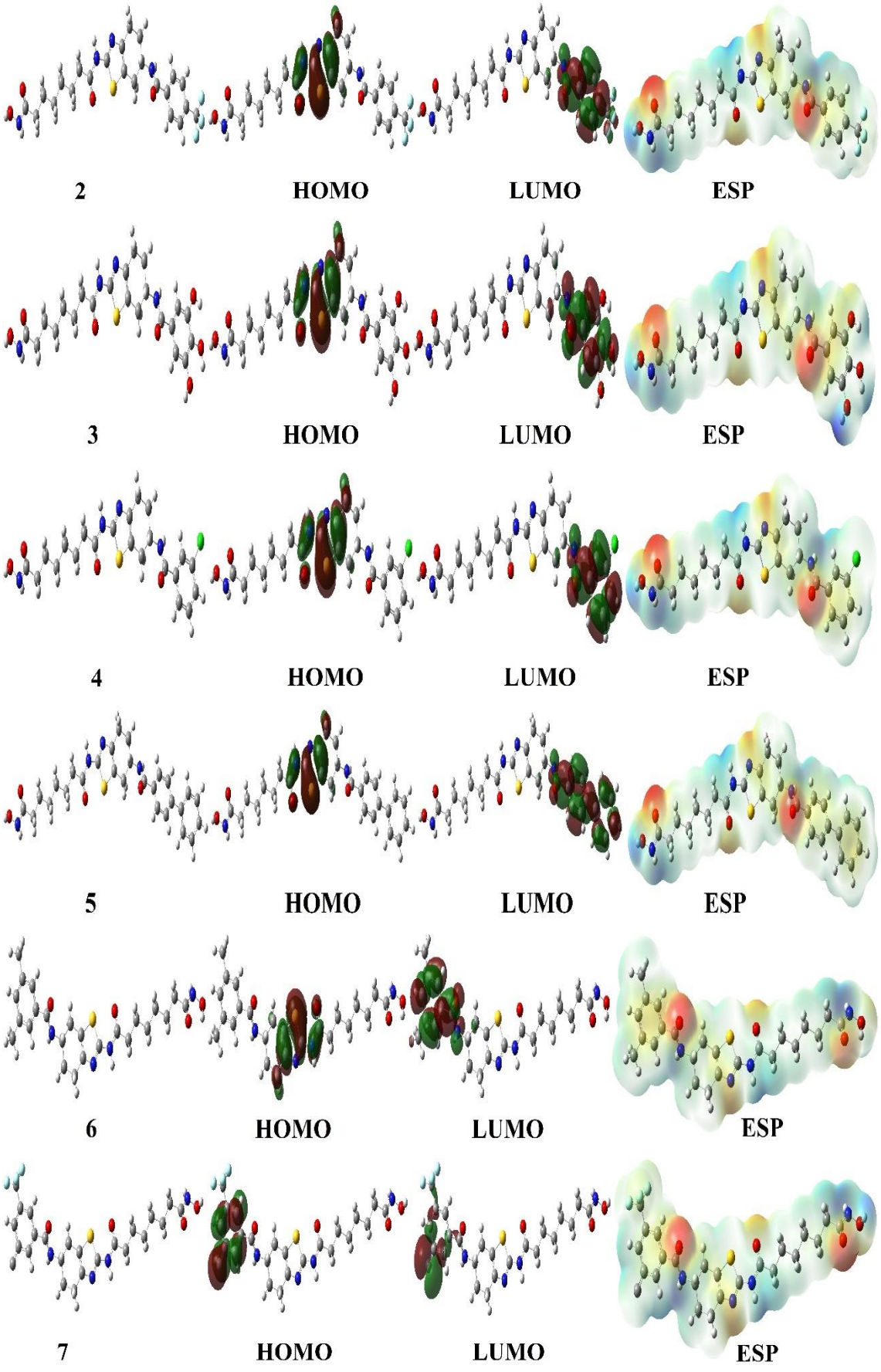
2
HOMO
LUMO
ESP
3
HOMO
LUMO
ESP
4
HOMO
LUMO
ESP
5
HOMO
LUMO
ESP
6
HOMO
LUMO
ESP
7
HOMO
LUMO
ESP

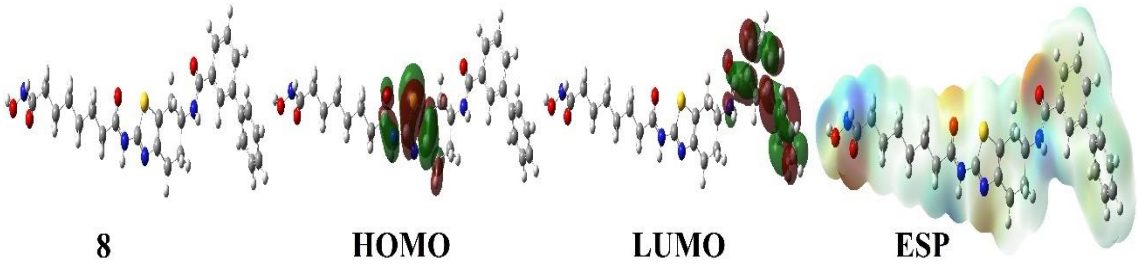

Figure 2. Representations of optimize structure, HOMO, LUMO, and ESP of molecules

In this study, the quantum chemical parameters calculated at the HF/6-31++G(d,p) level of eight different molecules were investigated. The calculated parameters include HOMO and LUMO energy levels, energy gap (ΔE), chemical hardness (η), softness (ε), chemical potential (μ), electronegativity (χ), electrophilicity index (ω), dipole moment and total energy values. These parameters were used to evaluate the electronic properties, reactivity and stability levels of the molecules.

HOMO and LUMO energy levels indicate the electron donation and acceptance tendencies of the molecules, respectively. HOMO values were calculated between –8.1798 and –8.5681 eV, and LUMO values were calculated between 0.6267 and 0.9851 eV. HOMO-LUMO energy gaps (ΔE) indicate the chemical stability and reactivity of the molecules. The lowest ΔE value was calculated for molecule number 7 (9.1948 eV), while the highest ΔE value was calculated for molecule number 4 (9.4416 eV). These data show that molecule number 7 is more reactive and molecule number 4 is more stable.

Chemical hardness (η) is calculated as half of ΔE and shows the resistance of molecules to external effects. The highest hardness value was again observed for molecule 4 (4.7208 eV), while the lowest hardness value was observed for molecule 7 (4.5974 eV). In contrast to hardness, chemical softness (ε) was calculated for molecule 7 at the highest value (0.5832), confirming once again that this molecule is highly reactive.

Chemical potential (μ) and electronegativity (χ) parameters define the degree of interaction of molecules with electrons. μ values range from 0.2118 to 0.2197 eV, and χ values range from 3.6279 to 3.9707 eV. When evaluated in terms of electronegativity, molecule 7 has the highest χ value (3.9707 eV). Parallel affinity (PA) is the negative value of electronegativity and represents the tendency to form bonds. Molecule 7 stands out as the structure with the highest PA value and the highest tendency to form bonds.

Electrophilicity index (ω) indicates the potential of a molecule to interact with nucleophilic systems. Molecule 7 has the highest electrophilicity index (1.7147 eV), indicating that it has a high probability of forming strong interactions with nucleophiles. The lowest ω value was calculated for molecule 1 (1.4457 eV).

Dipole moment is an important parameter indicating the polarity of molecules. Structures with high dipole moments tend to interact better with polar solvents. The highest dipole moment value was observed in molecule 6 (6.1349 Debye), while the lowest value was calculated in molecule 3 (3.2211 Debye). This suggests that molecule 6 has the most polar structure and may exhibit higher solubility in biological environments.

The total energy values of the molecules indicate their thermodynamic stability. The lowest total energy is molecule 2 (–57129.3047 a.u.), which makes it the most stable structure. The highest total energy value is in molecule 6 (–50119.5402 a.u.), which shows a less stable feature.

When evaluated in general, molecule 4 draws attention with its chemical stability, while molecule 7 draws attention with its high reactivity, softness, electrophilicity and electronegativity. While molecule 6 exhibits an advantageous structure in terms of solubility and biological interaction due to its high polarity, molecule 2 stands out as the most stable compound in terms of total energy value. These analyses reveal that the structural properties of these compounds have significant effects on their electronic distributions and potential biological activities.

Table 2. Numerical values of the docking parameters of molecule against protein

2VSM	Docking Score	Glide ligand efficiency	Glide hbond	Glide evdw	Glide ecoul	Glide emodel	Glide energy	Glide einternal	Glide posenum
1	-	-	-	-	-	-	-	-	-
2	-4.20	-0.12	-0.44	-38.77	-14.38	-56.41	-53.16	12.53	218
3	-5.75	-0.17	-0.32	-38.31	-17.30	-72.69	-55.61	5.04	241
4	-4.63	-0.14	-0.30	-40.88	-8.84	-63.45	-49.72	4.78	277
5	-4.52	-0.12	-0.60	-49.13	-8.91	-60.74	-58.04	13.64	299
6	-4.98	-0.15	-0.53	-38.20	-9.55	-59.01	-47.74	7.28	239
7	-5.30	-0.15	-0.73	-40.12	-12.64	-59.92	-52.76	10.13	207
8	-5.48	-0.15	-0.29	-43.56	-12.27	-69.20	-55.83	8.32	278
4CO6	Docking Score	Glide ligand efficiency	Glide hbond	Glide evdw	Glide ecoul	Glide emodel	Glide energy	Glide einternal	Glide posenum
1	-	-	-	-	-	-	-	-	-
2	-6.14	-0.18	-0.19	-42.85	-12.33	-77.67	-55.17	5.61	363
3	-5.91	-0.17	-0.43	-43.41	-12.89	-76.10	-56.30	9.07	373
4	-6.17	-0.19	-0.45	-44.56	-13.43	-78.53	-57.99	10.60	216
5	-8.09	-0.22	-0.30	-43.37	-15.91	-85.14	-59.28	9.35	107
6	-6.51	-0.20	-0.57	-44.04	-14.79	-81.52	-58.84	8.93	242
7	-6.42	-0.18	-0.73	-43.48	-14.84	-80.03	-58.32	9.34	144
8	-7.27	-0.20	-0.28	-47.75	-16.96	-90.48	-64.71	15.56	344

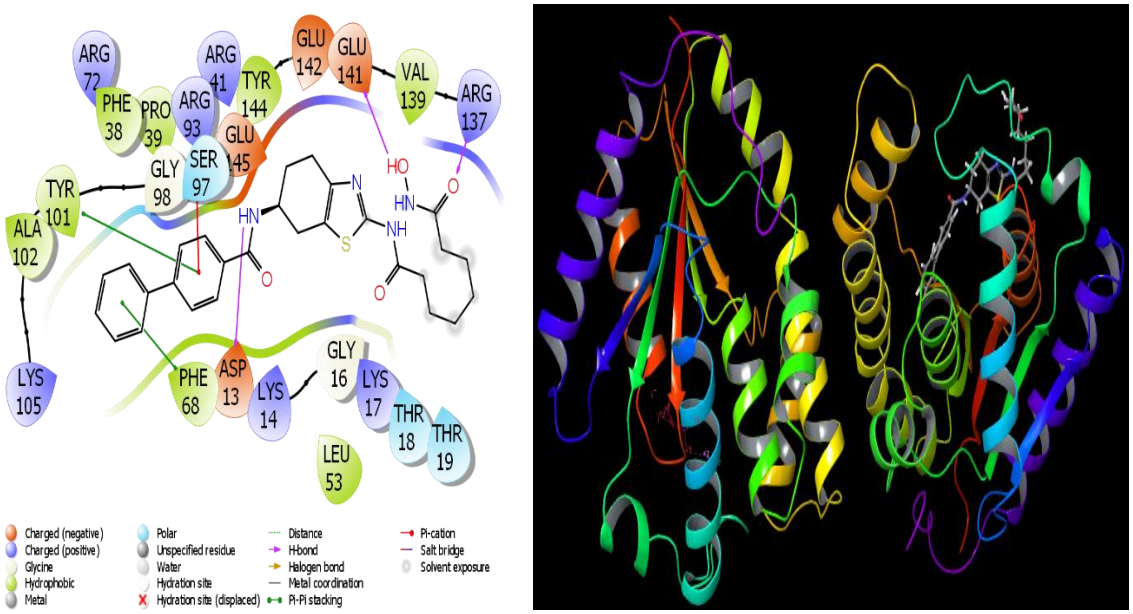

Figure 3. Presentation interactions of molecule 5 with 2V54 protein

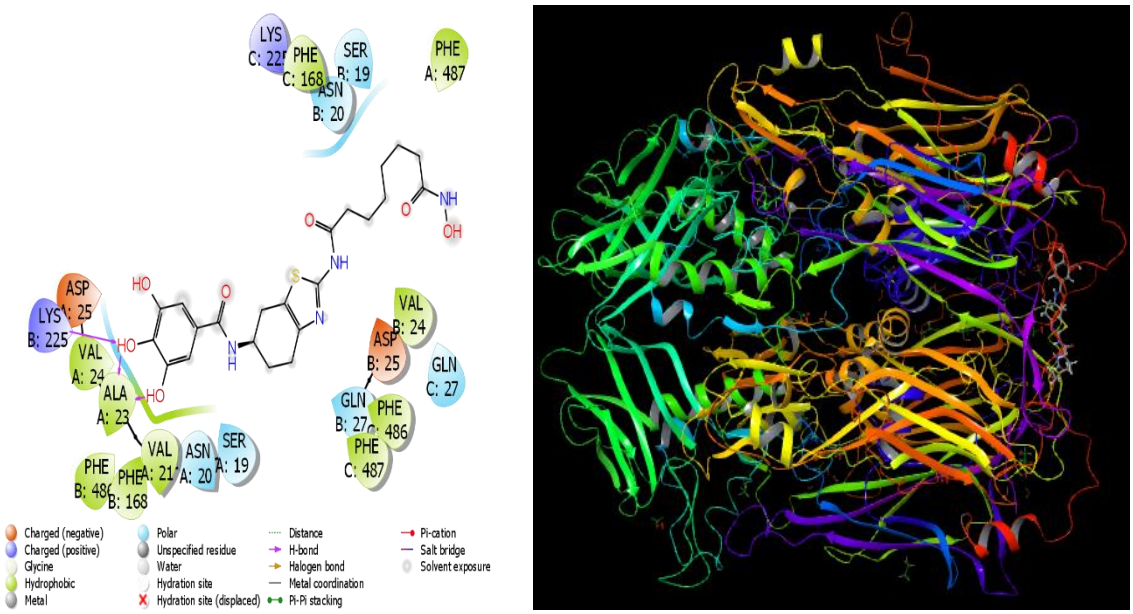

Figure 4. Presentation interactions of molecule 3 with 6BED protein

As a consequence of the broad use of theoretical research and technical developments, recent study reveals that the comparison of the biological activities of molecules has been greatly expedited and made easier [41]. This is a result of the fact that technology advancements have been made widely available. These two approaches of study have been applied to a significant degree, which has resulted in this being the outcome. This assumption receives support from the results of the most current study that has been conducted. The procedure of deciding which treatments are the most successful and effective prior to the testing of such medications in experimental settings has been greatly sped up and simplified as a result of calculations [42]. During the course of the theoretical calculations, a number of different elements were brought to light. Utilizing this approach allows for the determination of the nature of the link that exists between the numerical values of these parameters and the functioning of molecules in biological systems. This connection is discovered via the use of this method. This procedure is carried out in order to ensure that the biological parameters are evaluated properly. There are a number of factors that have an influence on the activities that have been described there [43], but the most essential aspect is the interactions that take place between various proteins and chemicals. As a consequence of the fact that these interactions are so widely dispersed, the proteins are eventually blocked. This specific mechanism is responsible for the inhibitory process that you are experiencing. The manner in which chemicals interact with a protein is what determines the amount of energy that the protein contains. Different types of interactions between molecules and proteins include hydrogen bonds, polar and hydrophobic contacts, π-π interactions, and halogen interactions [44-46]. These interactions may be classified into many categories. It is very necessary for molecules to interact with one another in order to keep the equilibrium at a consistent level. Numerous in-depth examinations into these chemical interactions have shown that there are a great many different ways in which proteins and chemicals interact with one another. This has been discovered during the course of these investigations. However, all of the figures can be found in Figures 3 and 4, and Table 2 includes all of the features. Figures 3 and 4 respectively include all of the figures.

After doing molecular docking simulations, the Glide ligand efficiency estimate is the most significant parameter that is determined from the simulations. Not only are these features complementary to one another, but there are many more. This numerical chart provides an indication of how efficiently the ligand acts against certain bacterial proteins. A specific example of this may be found here. Through the utilization of the Glide

Hbond [47], it is practicable to ascertain the quantity of hydrogen bonds that are produced as a consequence of the interactions that take place between molecules and proteins. In addition to being a statistic that illustrates the manner in which chemicals and proteins interact with one another, the Van der Waals interaction number, which is also widely referred to as Glide Evdw [48], is one of the statistics that illustrates these interactions. Glide Ecoul is a metric that is applied in order to perform an objective assessment of the Coulomb interactions that take place between medicines and proteins. This evaluation is carried out in order to ensure that the evaluation is objective. The Glide Einternal is the last parameter that is achieved as a consequence of these calculations. It is a numerical value that is acquired by integrating a large number of components [49]. Once this parameter is attained, the computations are complete.

Table 3. ADME properties of molecule

	1	**2**	**3**	**4**	**5**	**6**	**7**	**8**	**Referance Range**
mol_MW	-	513	493	479	521	473	527	521	130-725
dipole (D)	-	3.4	6.4	5.8	6.1	5.4	4.1	5.8	1.0-12.5
SASA	-	888	873	860	965	897	920	963	300-1000
FOSA	-	325	324	324	324	508	414	324	0-750
FISA	-	254	404	254	254	251	254	253	7-330
PISA	-	149	101	167	344	101	92	343	0-450
WPSA	-	161	43	115	43	37	161	43	0-175
volume (A^3)	-	1548	1518	1493	1694	1569	1607	1692	500-2000
donorHB	-	4	7	4	4	4	4	4	0-6
accptHB	-	10.7	12.9	10.7	10.7	10.7	10.7	10.7	2.0-20.0
glob (Sphere =1)	-	0.7	0.7	0.7	0.7	0.7	0.7	0.7	0.75-0.95
QPpolrz (A^3)	-	50.1	46.6	48.1	57.2	50.5	52.0	57.1	13.0-70.0
QPlogPC16	-	16.5	18.3	17.3	20.2	17.0	16.7	20.2	4.0-18.0
QPlogPoct	-	29.1	33.7	28.4	31.4	28.7	29.7	31.4	8.0-35.0
QPlogPw	-	21.1	27.6	21.1	22.3	20.6	20.7	22.3	4.0-45.0
QPlogPo/w	-	2.5	-0.6	2.0	3.1	2.1	2.7	3.1	-2.0-6.5
QPlogS	-	-6.1	-3.9	-5.4	-6.7	-5.7	-6.6	-6.6	-6.5-0.5
CIQPlogS	-	-5.2	-3.8	-4.6	-5.7	-4.4	-5.5	-5.7	-6.5-0.5
QPlogHERG	-	-5.3	-5.0	-5.3	-6.5	-5.0	-5.1	-6.4	*
QPPCaco (nm/sec)	-	21	1	21	21	23	21	21	**
QPlogBB	-	-2.9	-5.2	-3.0	-3.4	-3.2	-3.0	-3.4	-3.0-1.2
QPPMDCK (nm/sec)	-	113	1	63	25	25	113	26	**
QPlogKp	-	-4.6	-7.3	-4.5	-3.8	-4.7	-4.8	-3.8	Kp in cm/hr
IP (ev)	-	9.7	9.6	9.6	9.6	9.7	9.7	9.6	7.9-10.5
EA (eV)	-	0.8	0.7	0.7	0.6	0.7	0.7	0.6	-0.9-1.7
#metab	-	5	8	5	5	7	7	5	1-8
QPlogKhsa	-	-0.2	-0.9	-0.4	0.1	-0.2	-0.1	0.1	-1.5-1.5
Human Oral Absorption	-	2	1	2	1	2	1	1	-
Percent Human Oral Absor.	-	52	0	62	56	63	54	56	***
PSA	-	158	225	158	158	158	158	158	7-200
RuleOfFive	-	1	2	0	1	0	1	1	Maximum is 4
RuleOfThree	-	2	2	1	2	3	3	2	Maximum is 3
Jm	-	$1\ 10^{-05}$	$3\ 10^{-06}$	$5\ 10^{-05}$	$2\ 10^{-05}$	$2\ 10^{-05}$	$2\ 10^{-06}$	$2\ 10^{-05}$	-

In this study, ADME/T properties of eight different molecules were calculated using the Schrödinger QikProp module and their drug-like behaviors were evaluated in terms of pharmacokinetics. In order to understand the suitability of the molecules as drug candidates, various physicochemical, structural and bioavailability parameters were examined together with reference intervals.

Molecular weight (mol_MW) values were between 479–527 g/mol in all compounds, which is in line

with the recommended range of 130–725. This shows that all structures have molecular sizes in accordance with Lipinski rules. Dipole moment values range between 3.4 and 6.1 Debye. Especially molecule 6 (6.1 D) and molecule 5 (6.1 D) show high polarity, which provides advantage in terms of solubility in aqueous media.

SASA (total surface area) values from the surface area parameters were between 817–963 Å² and within the ideal range of 300–1000 Å². When parameters such as FISA (hydrophilic area) and PSA (polar surface area) were evaluated, the highest PSA value was observed in molecule 7 (184 Å²), indicating a more hydrophilic character. However, PSA above 140–150 Å² generally indicates poor cell permeability.

When the hydrogen bonding capacity was evaluated, donorHB and acceptHB parameters ranged between 4.0–4.3 and 10.6–12.9, respectively. Molecule 3 has the highest number of H-bond acceptor groups (12.9), which may be important in solubility and protein interactions.

When QPPCaco and QPPMDCK, which are among the parameters related to intestinal permeability, were evaluated, molecule 3 (QPPCaco: 89, QPPMDCK: 84 nm/s) had the highest values in these parameters and showed the highest bioavailability. On the other hand, the Caco-2 permeability (21.2 nm/s) of molecule 7 is low, indicating poor intestinal absorption. Similarly, the QPlogBB (blood-brain barrier permeability) value is -3.9 for molecule 7, which is also low; this indicates that the molecule is not suitable for being a central nervous system-targeted drug.

The QPlogHERG values associated with cardiotoxicity are between -5.0 and -5.7 and remain at or below the -5.0 limit, which is considered safe. This shows that the molecules have a safe profile in terms of the risk of HERG K^+ channel inhibition.

When the solubility-related parameters such as QPlogS and CIQPlogS are evaluated, the values ranging from -3.3 to -5.4 indicate that all molecules have moderate solubility in water. Molecule 3 stands out as the structure with the best solubility with a value of -3.3.

The Human Oral Absorption rate is "2" for all molecules, indicating moderate absorption. When evaluated as a percentage, molecule 8 (66%) has the highest oral absorption, while molecule 7 (40%) has the lowest. This indicates that molecule 7 may have limited bioavailability. Finally, when evaluated in terms of Lipinski's Rule of Five and Rule of Three, most of the molecules show 0 or 1 violation, which supports their potential to be a good drug candidate.

4. Conclusions

In conclusion, the integration of quantum chemical calculations, molecular docking, and ADME/T analyses has enabled a comprehensive in silico evaluation of octanediamide derivatives against monkeypox virus targets. Among the analyzed compounds, molecule 7 displayed the highest reactivity and electrophilicity, indicating a strong potential for biological activity. Molecule 4 stood out with its high chemical hardness and stability, whereas molecule 6 exhibited the highest dipole moment, suggesting enhanced solubility in polar environments. Molecular docking results identified molecules 5 and 8 as having the strongest protein-ligand binding affinities, particularly with the 4CO6 target. In terms of pharmacokinetics, molecule 3 demonstrated optimal oral absorption, membrane permeability, and solubility profiles, highlighting its suitability as a drug-like candidate. Overall, this study provides valuable insights into the antiviral potential of these molecules and identifies promising candidates for further experimental validation in the development of monkeypox virus inhibitors.

ACKNOWLEDGEMENT

The numerical calculations reported in this paper were fully/partially performed at TUBITAK ULAKBIM, High Performance and Grid Computing Center (TRUBA resources). This work was supported by the Scientific Research Project Fund of Sivas Cumhuriyet University (CUBAP) under the project number RGD-020.

References

[1] C.T. Cho, H.A. Wenner, Monkeypox virus. Bacteriological Reviews, 37(1) (1973) 1–18.

[2] A. Letafati, T. Sakhavarz, Monkeypox virus: A review. Microbial Pathogenesis, 176 (2023) 106027.

[3] D. Ulaeto, A. Agafonov, J. Burchfield, L. Carter, C. Happi, R. Jakob, ... R.F. Lewis, New nomenclature for mpox (monkeypox) and monkeypox virus clades. The Lancet. Infectious Diseases, 23(3) (2023) 273.

[4] W.J. Jorgensen, E.M. Duffy, Prediction of drug solubility from structure. Advanced

Drug Delivery Reviews, 54(3) (2002) 355–366.

[5] E. Lansiaux, N. Jain, S. Laivacuma, A. Reinis, The virology of human monkeypox virus (hMPXV): A brief overview. Virus Research, 322 (2022) 198932.

[6] E. Alakunle, U. Moens, G. Nchinda, M.I. Okeke, Monkeypox virus in Nigeria: infection biology, epidemiology, and evolution. Viruses, 12(11) (2020) 1257.

[7] M. Shafaati, M. Zandi, Human monkeypox (hMPXV) re-emergence: Host immunity status and current vaccines landscape. Journal of Medical Virology, 95(1) (2023) e28251.

[8] H. Karataş, H.K. Kiliç, B. Tüzün, Z. Kökbudak, Schiff base derivatives against monkeypox virus: Synthesis, in silico, MM-GBSA and SAR properties. Journal of Molecular Structure, 1298 (2024) 137073.

[9] S. Akash, S.A. Mir, S. Mahmood, S. Hossain, M.R. Islam, N. Mukerjee, ... M. Bourhia, Novel computational and drug design strategies for inhibition of monkeypox virus and Babesia microti: molecular docking, molecular dynamic simulation and drug design approach by natural compounds. Frontiers in Microbiology, 14 (2023) 1206816.

[10] H. Yalazan, D. Koç, F.A. Kose, M.İ. Akgül, S. Fandaklı, B. Tüzün, ... H. Kantekin, Chalcone-based schiff bases: Design, synthesis, structural characterization and biological effects. Journal of Molecular Structure, 1337 (2025) 142211.

[11] K. Pakkanen, From endosomes onwards: membranes, lysosomes and viral capsid interactions. University of Jyväskylä (2009) No. 203.

[12] S. Rampersad, P. Tennant, Replication and expression strategies of viruses. Viruses (2018) 55.

[13] N.L. Cianciola, S. Chung, D. Manor, C.R. Carlin, Adenovirus modulates toll-like receptor 4 signaling by reprogramming ORP1L-VAP protein contacts for cholesterol transport from endosomes to the endoplasmic reticulum. Journal of Virology, 91(6) (2017) 10-1128.

[14] D. Kazlauskas, M. Krupovic, Č. Venclovas, The logic of DNA replication in double-stranded DNA viruses: insights from global analysis of viral genomes. Nucleic Acids Research, 44(10) (2016) 4551–4564.

[15] L.G. Milroy, T.N. Grossmann, S. Hennig, L. Brunsveld, C. Ottmann, Modulators of protein–protein interactions. Chemical Reviews, 114(9) (2014) 4695–4748.

[16] S. Sun, W. Zhao, Y. Li, Z. Chi, X. Fang, Q. Wang, ... Y. Luan, Design, synthesis and antitumor activity evaluation of novel HDAC inhibitors with tetrahydrobenzothiazole as the skeleton. Bioorganic Chemistry, 108 (2021) 104652.

[17] D. Vautherin, D.T. Brink, Hartree-Fock calculations with Skyrme's interaction. I. Spherical nuclei. Physical Review C, 5(3) (1972) 626.

[18] C. Caillat, D. Topalis, L.A. Agrofoglio, S. Pochet, J. Balzarini, D. Deville-Bonne, P. Meyer, Crystal structure of poxvirus thymidylate kinase: an unexpected dimerization has implications for antiviral therapy. Proceedings of the National Academy of Sciences, 105(44) (2008) 16900–16905.

[19] D. Garriga, S. Headey, C. Accurso, M. Gunzburg, M. Scanlon, F. Coulibaly, Structural basis for the inhibition of poxvirus assembly by the antibiotic rifampicin. Proceedings of the National Academy of Sciences, 115(33) (2018) 8424–8429.

[20] R. Dennington, T.A. Keith, J.M. Millam, GaussView 6.0, Semichem Inc., Shawnee Mission, KS, USA (2016).

[21] M.J. Frisch, G.W. Trucks, H.B. Schlegel, G.R. Scuseria, M.A. Robb, J.R. Cheeseman, G. Scalmani, V. Barone, B. Mennucci, G.A. Petersson, ... D.J. Fox, Gaussian 09, revision D.01. Gaussian Inc., Wallingford (2009).

[22] A.E.M.A. Allah, S. Mortada, B. Tüzün, W. Guerrab, M. Qostal, J.T. Mague, ... Y. Ramli, Novel thiohydantoin derivatives: design, synthesis, spectroscopic characterization, crystal structure, SAR, DFT, molecular docking, pharmacological and toxicological activities. Journal of Molecular Structure, 1335 (2025) 141995.

[23] M. Dahmani, A. Titi, S. Kadri, A. ET-Touhami, A. Yahyi, B. Tüzün, ... I. Warad, Synthesis of two new Sn (IV) carboxylate complexes: Crystal structures, density

functional theory and Hirshfeld surface analysis computation, antibacterial, antifungal, and bioinformatics potential determination. Inorganic Chemistry Communications (2025) 114683.

[24] Schrödinger Release 2022-4: Maestro. Schrödinger, LLC, New York, NY, 2022.

[25] Schrödinger Release 2022-4: Protein Preparation Wizard; Epik; Impact; Prime. Schrödinger, LLC, New York, NY, 2022.

[26] Schrödinger Release 2022-4: LigPrep. Schrödinger, LLC, New York, NY, 2022.

[27] I. Shahzadi, A.F. Zahoor, B. Tüzün, A. Mansha, M.N. Anjum, A. Rasul, ... M. Mojzych, Repositioning of acefylline as anti-cancer drug: Synthesis, anticancer and computational studies of azomethines derived from acefylline tethered 4-amino-3-mercapto-1,2,4-triazole. PLOS ONE, 17(12) (2022) e0278027.

[28] M. El Faydy, L. Lakhrissi, N. Dahaieh, K. Ounine, B. Tüzün, N. Chahboun, ... A. Zarrouk, Synthesis, biological properties, and molecular docking study of novel 1,2,3-triazole-8-quinolinol hybrids. ACS Omega, 9(23) (2024) 25395–25409.

[29] Schrödinger Release 2022-4: QikProp. Schrödinger, LLC, New York, NY, 2022.

[30] E. Gorgun, A. Ali, M.S. Islam, Biocomposites of poly (lactic acid) and microcrystalline cellulose: influence of the coupling agent on thermomechanical and absorption characteristics. ACS Omega, 9(10) (2024) 11523–11533.

[31] S. Gürdaş Mazlum, D. Lodos, Modelling of Rheological Behaviour of Persimmon Puree. Turkish Journal of Agriculture - Food Science and Technology, 13(2) (2025) 439–445.

[32] H. Medetalibeyoğlu, A. Atalay, R. Sağlamtaş, S. Manap, A.B. Ortaakarsu, E. Ekinci, ... B. Tüzün, Synthesis, design, and cholinesterase inhibitory activity of novel 1,2,4-triazole Schiff bases: A combined experimental and computational approach. International Journal of Biological Macromolecules, 306 (2025) 141350.

[33] B. Tüzün, T. Agbektas, F.N. Naghiyev, A. Tas, C. Zontul, U. Ozum, ... I.G. Mamedov, In vitro cytotoxicity, gene expression, bioinformatics, biochemical analysis, and in silico analysis of synthesized carbonitrile derivatives. Monatshefte für Chemie - Chemical Monthly (2025) 1–22.

[34] A. Bouabbadi, M. Rbaa, B. Tüzün, A. Hmada, K. Dahmani, O. Kharbouch, ... M. Harcharras, Novel 8-hydroxyquinoline compounds used to inhibit mild steel corrosion in the presence of hydrochloric acid 1.0 M: an experimental and theoretical electrochemical study. Canadian Metallurgical Quarterly (2025) 1–18.

[35] T. Schrader, J. Khanifaev, E. Perlt, Koopmans' theorem for acidic protons. Chemical Communications, 59(93) (2023) 13839–13842.

[36] R.G. Pearson, Hard and soft acids and bases. Journal of the American Chemical Society, 85(22) (1963) 3533–3539.

[37] R.G. Pearson, Hard and soft acids and bases. Journal of the American Chemical Society, 85(22) (1963) 3533–3539.

[38] R.G. Parr, P.K. Chattaraj, Principle of maximum hardness. Journal of the American Chemical Society, 113(5) (1991) 1854–1855.

[39] P.W. Ayers, An elementary derivation of the hard/soft-acid/base principle. The Journal of Chemical Physics, 122(14) (2005).

[40] J.C. Phillips, Generalized Koopmans' Theorem. Physical Review, 123(2) (1961) 420.

[41] G. Güçlü, B. Tüzün, E. Uçar, N. Eruygur, M. Ataş, M. İnanır, ... B. Coşge Şenkal, Phytochemical and biological activity evaluation of Globularia orientalis L. Korean Journal of Chemical Engineering (2025) 1–17.

[42] B. Tüzün, T. Agbektas, F.N. Naghiyev, A. Tas, C. Zontul, U. Ozum, ... I.G. Mamedov, In vitro cytotoxicity, gene expression, bioinformatics, biochemical analysis, and in silico analysis of synthesized carbonitrile derivatives. Monatshefte für Chemie - Chemical Monthly (2025) 1–22.

[43] A. Bouabbadi, M. Rbaa, B. Tüzün, A. Hmada, K. Dahmani, O. Kharbouch, ... M. Harcharras, Novel 8-hydroxyquinoline compounds used to inhibit mild steel corrosion in the presence of hydrochloric acid 1.0 M: an experimental and theoretical

electrochemical study. Canadian Metallurgical Quarterly (2025) 1–18.

[44] N. Maliyakkal, P. Taslimi, B. Tüzün, S. Menadi, E. Cacan, A.A. Beeran, ... B. Mathew, Cholinesterase inhibition and anticancer properties of [4-(benzyloxy)phenyl]{methylidene}hydrazinylidene]-1,3-dihydro-2H-indol-2-ones using Swiss Target-guided prediction. Current Computer-Aided Drug Design (2025).

[45] U.A. Cevik, H. Ünver, H.E. Bostancı, B. Tüzün, N.İ. Gedik, Ü.M. Kocyigit, New hydrazone derivatives: synthesis, characterization, carbonic anhydrase I-II enzyme inhibition, anticancer activity and in silico studies. Zeitschrift für Naturforschung C (2025).

[46] H. Karatas, İ.B. Kul, M. Aydin, B. Tüzün, P. Taslimi, Z. Kokbudak, Alzheimer's disease drug design by synthesis, characterization, enzyme inhibition, in silico, SAR analysis and MM-GBSA analysis of Schiff bases derivatives. Korean Journal of Chemical Engineering (2025) 1–19.

[47] B. Tüzün, Evaluation of cytotoxicity, chemical composition, antioxidant potential, apoptosis relationship, molecular docking, and MM-GBSA analysis of Rumex crispus leaf extracts. Journal of Molecular Structure, 1323 (2025) 140791.

[48] M. Akkus, M. Kirici, A. Poustforoosh, M.K. Erdogan, R. Gundogdu, B. Tüzün, P. Taslimi, Phenolic compounds: Investigating their anti-carbonic anhydrase, anti-cholinesterase, anticancer, anticholinergic, and antiepileptic properties through molecular docking, MM-GBSA, and dynamics analyses. Korean Journal of Chemical Engineering (2025) 1–20.

[49] N. Ullah, A. Alam, B. Tüzün, N.U. Rehman, M. Ayaz, A.A. Elhenawy, ... M. Ahmad, Synthesis of novel thiazole derivatives containing 3-methylthiophene carbaldehyde as potent anti α-glucosidase agents: In vitro evaluation, molecular docking, dynamics, MM-GBSA, and DFT studies. Journal of Molecular Structure, 1321 (2025) 140070.

[50] S. Çiçek, Y.B. Korkmaz, B. Tüzün, S. Işik, M.T. Yilmaz, F. Özoğul, A study on insecticidal activity of the fennel (Foeniculum vulgare) essential oil and its nanoemulsion against stored product pests and molecular docking evaluation. Industrial Crops and Products, 222 (2024) 119859.

[51] S. Kapancık, M.S. Çelik, M. Demiralp, K. Ünal, S. Çetinkaya, B. Tüzün, Chemical composition, cytotoxicity, and molecular docking analyses of Thuja orientalis extracts. Journal of Molecular Structure, 1318 (2024) 139279.

[52] S. Manap, H. Medetalibeyoğlu, A. Kılıç, O.F. Karataş, B. Tüzün, M. Alkan, ... H. Yüksek, Synthesis, molecular modeling investigation, molecular dynamic and ADME prediction of some novel Mannich bases derived from 1,2,4-triazole, and assessment of their anticancer activity. Journal of Biomolecular Structure and Dynamics, 42(21) (2024) 11916–11930.

[53] O. Myroslava, A. Poustforoosh, B. Inna, V. Parchenko, B. Tüzün, B. Gutyj, Molecular descriptors and in silico studies of 4-((5-(decylthio)-4-methyl-4n-1,2,4-triazol-3-yl)methyl)morpholine as a potential drug for the treatment of fungal pathologies. Computational Biology and Chemistry, 113 (2024) 108206.

[54] K. Ganbarov, A. Huseynzada, G. Binate, K. Sayin, N. Sadikhova, V. Ismailov, ... A. Algherbawi, Biological and in silico studies of methyl 2-(2-methoxy-2-oxoethyl)-4-methylfuran-3-carboxylate as a promising antimicrobial agent. Acta Scientiarum-Technology, 47(1) (2025).

[55] K. Prabha, S. Rajendran, B.M. Gnanamangai, K. Sayin, K.R. Prasad, G. Tüzün, Synthesis of novel isostere analogues of naphthyridines using CuI catalyst: DFT computations (FMO, MEP), molecular docking and ADME analysis. Tetrahedron, 168 (2024) 134323.

[56] A. Huseynzada, M. Mori, F. Meneghetti, A. Israyilova, G. Tuzun, K. Sayin, ... V. Abbasov, Synthesis, crystal structure, Hirshfeld surface, computational and antibacterial studies of a 9-phenanthrenecarboxaldehyde-based thiodihydropyrimidine derivative. Journal of Molecular Structure, 1267 (2022) 133571.

[57] A.H.T. Kafa, G. Tüzün, E. Güney, R. Aslan, K. Sayın, B. Tüzün, H. Ataseven, Synthesis, computational analyses, antibacterial and antibiofilm properties of nicotinamide

derivatives. Structural Chemistry, 33(4) (2022) 1189–1197.

[58] H. Yildiz, G. Tüzün, E. Erbayraktar, Sarı Kantoron (Hypericum perforatum) bitkisinin antioksidan ve antimikrobiyal özellikleri üzerine bir araştırma. ISPEC Journal of Science Institute, 1(1) (2022) 27–32.

[59] C.A. Lipinski, Lead-and drug-like compounds: the rule-of-five revolution. Drug Discovery Today: Technologies, 1(4) (2004) 337–341.

[60] C.A. Lipinski, F. Lombardo, B.W. Dominy, P.J. Feeney, Experimental and computational approaches to estimate solubility and permeability in drug discovery and development settings. Advanced Drug Delivery Reviews, 23 (1997) 3–25.

[61] W.J. Jorgensen, E.M. Duffy, Prediction of drug solubility from structure. Advanced Drug Delivery Reviews, 54(3) (2002) 355–366.